

# A comprehensive score reflecting memory-related fMRI activations and deactivations as potential biomarker for neurocognitive aging

Joram Soch<sup>1,2,\*</sup>, Anni Richter<sup>3,\*</sup>, Hartmut Schütze<sup>4,5</sup>, Jasmin M. Kizilirmak<sup>1</sup>, Anne Assmann<sup>4,5</sup>, Hannah Feldhoff<sup>3,5</sup>, Larissa Fischer<sup>3,5</sup>, Julius Heil<sup>3,5</sup>, Lea Knopf<sup>3,5</sup>, Christian Merkel<sup>3,5</sup>, Matthias Raschick<sup>3,5</sup>, Clara-Johanna Schietke<sup>3,5</sup>, Annika Schult<sup>3,5</sup>, Renat Yakupov<sup>4</sup>, Gabriel Ziegler<sup>4,5</sup>, Jens Wiltfang<sup>1,7</sup>, Emrah Düzel<sup>4,5,6</sup>, Björn H. Schott<sup>1,3,6,7</sup>

<sup>1</sup> German Center for Neurodegenerative Diseases (DZNE), Göttingen, Germany

<sup>2</sup> Bernstein Center for Computational Neuroscience (BCCN), Berlin, Germany

<sup>3</sup> Leibniz Institute for Neurobiology (LIN), Magdeburg, Germany

<sup>4</sup> German Center for Neurodegenerative Diseases (DZNE), Magdeburg, Germany

<sup>5</sup> Otto von Guericke University, Medical Faculty, Magdeburg, Germany

<sup>6</sup> Center for Behavioral Brain Sciences (CBBS), Magdeburg, Germany

<sup>7</sup> Department of Psychiatry and Psychotherapy, University Medical Center Göttingen, Göttingen, Germany

\* These authors contributed equally to this work.

## Address for correspondence:

Dr. Joram Soch

German Center for Neurodegenerative Diseases

Von-Siebold-Str. 3a

37075 Göttingen, Germany

[joram.soch@dzne.de](mailto:joram.soch@dzne.de) / [joram.soch@bccn-berlin.de](mailto:joram.soch@bccn-berlin.de)

PD Dr. Dr. Björn Hendrik Schott

Leibniz Institute for Neurobiology

Brenneckestr. 6

39118 Magdeburg, Germany

[bschott@lin-magdeburg.de](mailto:bschott@lin-magdeburg.de) / [bjoern-hendrik.schott@dzne.de](mailto:bjoern-hendrik.schott@dzne.de)

**Key words:** subsequent memory effect, episodic memory, fMRI, hippocampus, cognitive aging, memory impairment

## Abstract

Older adults and particularly those at risk for developing dementia typically show a decline in episodic memory performance, which has been associated with altered memory network activity detectable via functional magnetic resonance imaging (fMRI). To quantify the degree of these alterations, a score has been developed as a putative imaging biomarker for successful aging in memory for older adults (*Functional Activity Deviations during Encoding*, FADE; Düzel et al., 2011). Here, we introduce and validate a more comprehensive version of the FADE score, termed FADE-SAME (*Similarity of Activations during Memory Encoding*), which differs from the original FADE score by considering not only activations but also deactivations in fMRI contrasts of stimulus novelty and successful encoding, and by taking into account the variance of young adults' activations. We computed both scores for novelty and subsequent memory contrasts in a cohort of 217 healthy adults, including 106 young and 111 older participants, as well as a replication cohort of 117 young subjects. We further tested the stability and generalizability of both scores by controlling for different MR scanners and gender, as well as by using different data sets of young adults as reference samples. Both scores showed robust age-group-related differences for the subsequent memory contrast, and the FADE-SAME score additionally exhibited age-group-related differences for the novelty contrast. Furthermore, both scores correlate with behavioral measures of cognitive aging, namely memory performance. Taken together, our results suggest that single-value scores of memory-related fMRI responses may constitute promising biomarkers for quantifying neurocognitive aging.

## Outline

<b>1. Introduction</b> .....	4
<b>2. Methods</b> .....	7
<b>2.1. Participants</b> .....	7
<b>2.2. Experimental paradigm</b> .....	7
<b>2.3. fMRI data acquisition</b> .....	8
<b>2.4. fMRI data preprocessing</b> .....	8
<b>2.5. General linear modelling</b> .....	8
<b>2.6. Functional activity deviation during encoding (FADE-classic)</b> .....	9
<b>2.7. Similarities of activations during memory encoding (FADE-SAME)</b> .....	10
<b>2.8. Extraction of FADE-classic and FADE-SAME scores</b> .....	11
<b>2.9. Statistical evaluation of FADE-classic and FADE-SAME scores</b> .....	12
<b>2.10. Replication with an independent baseline cohort</b> .....	13
<b>3. Results</b> .....	14
<b>3.1. Age-related differences in the human memory network could be replicated</b> .....	14
<b>3.2. FADE scores are modulated by age, but neither gender nor MRI scanner</b> .....	14
<b>3.3. FADE scores differ in their ability to capture age-related differences</b> .....	15
<b>3.4. FADE scores correlate with other indices of cognitive aging</b> .....	17
<b>3.5. The FADE-SAME score is stable across different cohorts of young subjects</b> .....	18
<b>3.6. FADE scores are stable for older subjects when using different reference samples</b> ....	19
<b>4. Discussion</b> .....	21
<b>4.1. Different FADE scores as biomarkers of the aging memory system</b> .....	21
<b>4.2. Novelty and subsequent memory contrasts as basis for the FADE scores</b> .....	22
<b>4.3. Reductionist versus multi-voxel fMRI activation scores as potential biomarkers</b> .....	23
<b>4.4. Clinical implications and directions for future research</b> .....	25
<b>4.5. Conclusion</b> .....	25
<b>5. References</b> .....	27
<b>6. Appendix</b> .....	30
<b>A. Interpretations of the FADE-SAME score</b> .....	30
<b>B. Computation of memory performance</b> .....	31
<b>C. Computation of hippocampal volumes</b> .....	32
<b>7. Statements</b> .....	33
<b>7.1. Acknowledgments</b> .....	33
<b>7.2. Data Availability Statement</b> .....	33
<b>7.3. Funding and Conflict of Interest declaration</b> .....	33

## 1. Introduction

In functional magnetic resonance imaging (fMRI) studies of episodic memory, a widely used approach is to probe the successful acquisition of novel information (*encoding*) as a function of performance in a later memory test (*retrieval*), the so-called “subsequent memory effect” or difference due to later memory (DM) effect (Paller et al., 1987). Since its first application to fMRI (Brewer, 1998; Wagner et al., 1998), numerous studies have employed this approach, and meta-analytic evidence shows that successful encoding robustly engages the MTL as well as inferior temporal, prefrontal, and parietal cortices (Kim, 2011). Older individuals display characteristic alterations in memory-related network activations, including a reduced activation in the MTL, particularly the parahippocampal (PHC) cortex and a reduced deactivation or even atypical activation of midline cortical structures (Düzel et al., 2011; for a review and meta-analysis see Maillet and Rajah, 2014).

Age-related differences in the neuroanatomical underpinnings of successful episodic encoding are rather robust at the group level. However, few studies have explored the applicability of such age-related changes in encoding-related fMRI activations as an individual biomarker for cognitive aging. In one study specifically aimed at individual differences, Düzel and colleagues employed a reductionist approach, in which the age-related alterations of encoding-related network activations are described in a single number that denotes the degree of deviation from the prototypical activation pattern observed in young adults (*Functional Activity Deviation during Encoding*, FADE; Düzel et al., 2011). In the original study by Düzel and colleagues (2011), the FADE score was based on neural correlates of successful memory encoding, namely, the DM effect, but this approach may be limited in participants with poor memory performance, due to lack of successfully encoded items (Soch et al., 2020). To circumvent this limitation, one might base the FADE score calculation on the novelty effect, namely the brain’s response to novel information, irrespective of encoding success, an approach supported by recent observations that hippocampal novelty responses correlate with tau protein concentrations in cerebrospinal fluid (CSF) in older adults (Düzel et al., 2018). An alternative, or perhaps complementary, approach to focusing may be the use of a parametric model of the DM effect, which can also be computed in individuals with relatively poor memory performance (Soch et al., 2020). However, both approaches have not yet been used in the context of the FADE score and therefore warrant validation.

The aim of the present study was two-fold: On the one hand, we aimed to validate the use of a single numeric value reflecting memory-related fMRI activation differences as a proxy of

cognitive aging in a large cohort of healthy older participants, using both the novelty contrast and a parametric DM effect. Secondly, we aimed to extend the original FADE score (hence termed FADE-classic) by (i) considering both activations and deactivations during encoding and by (ii) taking into account the variance of the reference sample of young subjects required for its computation, thereby yielding the so-called FADE-SAME score (*Similarity of Activations during Memory Encoding*). Specifically, the following features were implemented:

- i) Both novelty and DM contrasts engage a similar set of brain regions, including the MTL with the PHC and hippocampus (HC), inferior temporo-occipital and lateral parietal cortices, and the dorsolateral prefrontal cortex (dlPFC) (Düzel et al., 2011; Soch et al., 2020). Collectively, these brain regions can be considered to constitute a human memory network. Notably, older subjects do not only show reduced activations in this network, particularly in the PHC, but also reduced *deactivations* in brain regions like the ventral precuneus and posterior cingulate cortex (PreCun/PCC; see Figure 2), which are part of the brain's default mode network (DMN) (Maillet & Rajah, 2014; S. L. Miller et al., 2008). These deactivations were already mentioned in the original study of the FADE score (Düzel et al., 2011) and are now explicitly considered when computing the FADE-SAME score.
- ii) The FADE score reflects, by definition, the deviation of an older adult's memory-related activation pattern from the prototypical pattern seen in young adults. It therefore requires referencing the activation map of the respective individual to a baseline activation map obtained from a cohort of young adults (Düzel et al., 2011). However, memory-related fMRI activation patterns also exhibit individual differences among young adults, which are stable over time and thus likely reflect traits (M. B. Miller et al., 2002). To avoid potential biases related to individual activation patterns of the specific young adults contributing to the FADE score template, it is thus advisable to account for the variance of the reference sample itself, which is implemented in the calculation of the FADE-SAME score.

To evaluate how both the classic FADE score and the FADE-SAME score perform as potential biomarkers of neurocognitive aging, we compared the two scores in a large sample of healthy young (N = 106; age range: 18-35 years) and older participants (N = 111; age

range: 60-80 years) studied within the *Autonomy in Old Age* project<sup>1</sup> (Assmann et al., 2020; Soch et al., 2020). This study used a shortened version of the subsequent memory paradigm from the original FADE study (Düzel et al., 2011), which is also employed in the DELCODE study, a large-scale longitudinal study of pre-clinical stages of Alzheimer's disease (AD) (Bainbridge et al., 2019; Düzel et al., 2018). In this paradigm, photographs of scenes are encoded incidentally via an indoor/outdoor decision task, and memory is tested via an old/new recognition memory task with a five-step confidence rating. The FADE-classic and FADE-SAME scores were computed on activation maps from both successful memory encoding (Düzel et al., 2011; Soch et al., 2020) and novelty processing (Düzel et al., 2018), and evaluated with respect to their power to differentiate between age groups and their correlation with memory performance and hippocampal volumes.

---

<sup>1</sup> The sample also included a smaller subgroup of middle-aged individuals (N = 42; age range: 51-59 years) who were of lesser interest for the current analyses, but whose data are reported in the Supplementary Material for completeness reasons.

## 2. Methods

### 2.1. Participants

The study cohort consisted of a total of 217 neurologically and psychiatrically healthy adults, including 106 young (47 male, 59 female, age range 18-35, mean age  $24.12 \pm 4.00$  years) and 111 older (46 male, 65 female, age range 60-80, mean age  $67.28 \pm 4.65$  years) participants. According to self-report, all participants were right-handed and did not use centrally acting medication. The Mini-International Neuropsychiatric Interview (M.I.N.I.; Sheehan et al., 1998; German version by Ackenheil et al., 1999) was used to exclude present or past psychiatric illness, alcohol or drug abuse. The study was approved by the Ethics Committee of the Otto von Guericke University Magdeburg, Faculty of Medicine, and written informed consent was obtained from all participants in accordance with the Declaration of Helsinki (World Medical Association, 2013).

### 2.2. Experimental paradigm

During the fMRI experiment, participants performed a visual memory encoding paradigm with an indoor/outdoor judgment as the incidental encoding task. Compared to earlier publications of this paradigm (Assmann et al., 2020; Barman et al., 2014; Düzel et al., 2011; Schott et al., 2014), the trial timings had been adapted as part of the DELCODE study protocol (Bainbridge et al., 2019; Düzel et al., 2018; Soch et al., 2020, for a detailed comparison of trial timings and acquisition parameters). Subjects viewed photographs showing indoor and outdoor scenes, which were either novel at the time of presentation (44 indoor and 44 outdoor scenes) or were repetitions of two highly familiar “master” images (one indoor and one outdoor scene pre-familiarized before the actual experiment). Participants were instructed to categorize images as “indoor” or “outdoor” via button press. Each picture was presented for 2.5 s, followed by a variable delay between 0.70 s and 2.65 s.

Approximately 70 minutes ( $70.19 \pm 3.60$  min) after the start of the fMRI session, subjects performed a computer-based recognition memory test outside the scanner, in which they were presented with photographs that were either shown during the fMRI encoding phase (*old*) or *new* to the participant. Participants rated each image on a five-point Likert scale from 1 (“definitely new”) to 5 (“definitely old”). For detailed experimental procedure, see Assmann et al. (2020) and Soch et al. (2020).

### 2.3. fMRI data acquisition

Structural and functional MRI data were acquired on two Siemens 3T MR tomographs (Siemens Verio: 58 young, 64 older; Siemens Skyra: 48 young, 47 older), following the exact same protocol used in the DELCODE study (Düzel et al., 2019; Jessen et al., 2018).

A T1-weighted MPRAGE image (TR = 2.5 s, TE = 4.37 ms, flip- $\alpha$  = 7°; 192 slices, 256 x 256 in-plane resolution, voxel size = 1 x 1 x 1 mm) was acquired for co-registration and improved spatial normalization. Phase and magnitude fieldmap images were acquired to improve correction for artifacts resulting from magnetic field inhomogeneities (*unwarping*, see below).

For functional MRI (fMRI), 206 T2\*-weighted echo-planar images (TR = 2.58 s, TE = 30 ms, flip- $\alpha$  = 80°; 47 slices, 64 x 64 in-plane resolution, voxel size = 3.5 x 3.5 x 3.5 mm) were acquired in interleaved-ascending slice order (1, 3, ..., 47, 2, 4, ..., 46). The total scanning time during the task-based fMRI session was approximately 530 s. The complete study protocol also included a T2-weighted MR image in perpendicular orientation to the hippocampal axis (TR = 3.5 s, TE = 350 ms, 64 slices, voxel size = 0.5 x 0.5 x 1.5 mm) for optimized segmentation of the hippocampus (see Appendix C) as well as resting-state fMRI (rs-fMRI) and additional structural imaging not used in the analyses reported here.

### 2.4. fMRI data preprocessing

Data preprocessing was performed using Statistical Parametric Mapping (SPM12; Wellcome Trust Center for Neuroimaging, University College London, London, UK). EPIs were corrected for acquisition time delay (*slice timing*), head motion (*realignment*) and magnetic field inhomogeneities (*unwarping*), using voxel-displacement maps (VDMs) derived from the fieldmaps. The MPRAGE image was spatially co-registered to the mean unwarped image and *segmented* into six tissue types, using the unified segmentation and normalization algorithm implemented in SPM12. The resulting forward deformation parameters were used to *normalize unwarped* EPIs into a standard stereotactic reference frame (Montreal Neurological Institute, MNI; voxel size = 3 x 3 x 3 mm). Normalized images were spatially *smoothed* using an isotropic Gaussian kernel of 6 mm full width at half maximum (FWHM).

### 2.5. General linear modelling

For first-level fMRI data analysis, which was also performed in SPM12, we used a parametric general linear model (GLM) of the subsequent memory effect that has recently been demonstrated to outperform the thus far more commonly employed categorical models of the fMRI subsequent memory effect (Soch et al., 2020).



This model included two onset regressors, one for novel images at the time of presentation (“novelty regressor”) and one for presentations of the two pre-familiarized images (“master regressor”). Both regressors were created as short box-car stimulus functions with an event duration of 2.5 s, convolved with the canonical hemodynamic response function, as implemented in SPM12.

The regressor reflecting subsequent memory performance was obtained by parametrically modulating the novelty regressor with a function describing subsequent memory report. Specifically, the parametric modulator (PM) was given by

$$PM = \arcsin\left(\frac{x - 3}{2}\right) \cdot \frac{2}{\pi}$$

where  $x \in \{1, 2, 3, 4, 5\}$  is the subsequent memory report, such that  $-1 \leq PM \leq +1$ . Compared to a linear-parametric model, this transformation puts a higher weight on definitely remembered (5) or forgotten (1) items compared with probably remembered (4) or forgotten (2) items (Soch et al., 2020, Fig. 2A).

The model also included the six rigid-body movement parameters obtained from realignment as covariates of no interest and a constant representing the implicit baseline.

## 2.6. Functional activity deviation during encoding (FADE-classic)

The original FADE score<sup>2</sup> (here: FADE-classic) constitutes the first implementation of a single-value score of encoding-related fMRI activations designed as a potential biomarker in age-related memory decline. Computation of classic FADE scores canonically proceeds in two steps (Düzel et al., 2011, p. 805) (see Figure 2):

1. First, a reference map is generated by submitting contrast maps from young subjects to a group-level analysis and determining the set of voxels in which there is a significant positive effect (e.g., memory contrast: higher activations for items later remembered vs. later forgotten), with the entire set of voxels considered a “volume of interest” (VOI).
2. Then, the same contrast is computed for each older subject, resulting in a t-value map for each subject. Finally, the FADE score is obtained by subtracting the average t-value inside the VOI from the average t-value outside the VOI.

More precisely, let  $J_+$  be the set of voxels showing a positive effect in young subjects at an *a priori* defined significance level ( $p < 0.001$ , uncorrected, minimum cluster size  $k = 6$  voxels in the original publication;  $p < 0.05$ , FWE-corrected, extent threshold  $k = 10$  in the present

---

<sup>2</sup> Colloquially, the memory experiment employed here is also called the “FADE paradigm” due to this score.

work), and let  $t_{ij}$  be the t-value of the  $i$ -th older subject in the  $j$ -th voxel. Then, the FADE score of this subject is given by

$$\text{FADE}_i = \frac{1}{v} \sum_{j \notin J_+} t_{ij} - \frac{1}{v_+} \sum_{j \in J_+} t_{ij}$$

where  $v_+$  and  $v$  is the number of voxels inside and outside  $J_+$ , respectively (see Figure 1B). While originally developed for the subsequent memory contrast (termed “recognition-encoding contrast” in the original publication), it is in principle also possible to calculate the score for the novelty contrast (novel images vs. familiar images). In either case, a larger FADE score signifies higher deviation of an older adult’s memory – or novelty – response from the prototypical response seen in young adults.

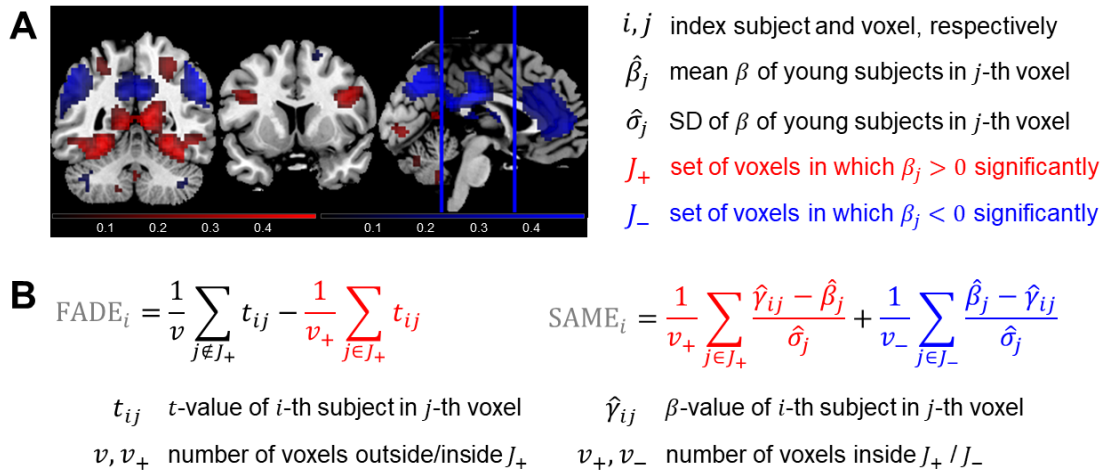


**Figure 1. Measures for quantifying successful aging in memory.** We compute two summary statistics from fMRI contrasts, which are both based on a group-level analysis across all young subjects and subject-wise computation in each older subject. **(A)** A reference map is obtained by significance testing of a contrast within the group of young subjects, resulting in voxels with significant activation (red) or significant deactivation (blue). **(B)** FADE-classic and FADE-SAME score of older subjects are calculated as summary statistics by averaging single-subject contrast outcomes within selected sets of voxels (for explanations, see text).

## 2.7. Similarities of activations during memory encoding (FADE-SAME)

In addition to evaluating the classic FADE score in a large cohort, we further developed the FADE-SAME score as a more comprehensive version of the FADE score, which was motivated based on the following considerations:

1. Older adults do not only deviate in encoding-related fMRI activity from young adults by reduced activations in voxels with a positive effect ( $J_+$ ), but also by reduced deactivations in voxels with a negative effect ( $J_-$ ) (see Figure 2; also see Maillet & Rajah, 2014).
2. The normalized activation loss, relative to young subjects, in one voxel is

$$(\hat{\gamma}_{ij} - \hat{\beta}_j) / \hat{\sigma}_j$$

and the normalized deactivation loss, relative to young subjects, in one voxel is

$$(\hat{\beta}_j - \hat{\gamma}_{ij}) / \hat{\sigma}_j$$

where  $\hat{\beta}_j$  is the average contrast estimate in young subjects,  $\hat{\sigma}_j$  is the standard deviation of young subjects on this contrast at the  $j$ -th voxel, and  $\hat{\gamma}_{ij}$  is the contrast estimate of the  $i$ -th older subject at the  $j$ -th voxel (see Figure 1).

3. The FADE-SAME score is obtained by averaging within the sets of voxels with positive and negative effect, respectively, and adding up the two components

$$\text{SAME}_i = \frac{1}{v_+} \sum_{j \in J_+} \frac{\hat{\gamma}_{ij} - \hat{\beta}_j}{\hat{\sigma}_j} + \frac{1}{v_-} \sum_{j \in J_-} \frac{\hat{\beta}_j - \hat{\gamma}_{ij}}{\hat{\sigma}_j}$$

where  $v_+$  and  $v_-$  are the numbers of voxels in  $J_+$  and  $J_-$ , respectively (see Figure 1B).

4. As becomes evident in this equation, the FADE-SAME score includes a correction for the standard deviation of the parameter estimates at any given voxel in the baseline cohort of young subjects. Thereby, voxels showing prototypical activation across the baseline cohort are weighted more strongly than those activating less robustly.

The FADE-SAME score allows for a number of interpretations (see Appendix A). Most generally, a higher FADE-SAME score indicates higher similarity of an older adult's brain responses with the activation and deactivation patterns seen in young subjects.

## 2.8. Extraction of FADE-classic and FADE-SAME scores

After single-subject model estimation, FADE-classic and FADE-SAME scores were calculated from t-values (FADE-classic; see Section 2.6) or estimated regression coefficients (FADE-SAME; see Section 2.7). For both the FADE-classic and the FADE-SAME score to be suitable as biomarkers for cognitive aging, it is important to assess to what extent these scores actually reflect age-related activation deviations rather than age-independent individual differences. To explore this potential caveat further, we computed both scores also for the young study participants. In order to avoid circularity issues when calculating scores for a given young subject – whose data were also used to generate reference maps –, the entire cohort was split into two cross-validation (CV) groups.

These CV groups were created by randomly splitting each cohort of subjects (young, older) and then testing whether the two groups significantly differ regarding mean age, gender ratio and scanner ratio. This procedure was repeated until the p-value for all three tests was larger than 0.5 and the final partition was reported for each cohort (see Supplementary Table S1). The resulting CV groups did not differ significantly with respect to (i) their mean age, (ii) the

number of male versus female subjects and (iii) the MRI scanner on which participants were investigated (Verio vs. Skyra). Then, scores of any given (young or older) participant in CV group 2 were calculated based on reference maps generated from all young subjects in CV group 1, and vice versa. For completeness, these calculations were also performed for the middle-aged subjects in our cohort (Soch et al., 2020), who were treated as a separate group and are reported in the supplement (see Supplementary Figure S1).

Using this procedure, FADE-classic and FADE-SAME scores were computed on the novelty contrast (novelty – master; contrast vector:  $c = [+1, 0, -1]^T$ ) and on the memory contrast (arcsine-transformed PM; contrast vector:  $c = [0, 1, 0]^T$ ), leading to 217 values (number of subjects) for each of the four scores (novelty vs. memory x FADE-classic vs. FADE-SAME) in total.

## 2.9. Statistical evaluation of FADE-classic and FADE-SAME scores

To investigate the robustness and utility of the two scores, the values calculated using the methods described above were subjected to a number of statistical evaluations:

- We first computed between-subject ANOVAs for all scores to test for potential effects of age group, scanner or gender.
- Next, mixed ANOVAs were computed for all scores to test for interactions of the within-subject factor score (FADE-classic vs. FADE-SAME) and the between-subject factor age group (young vs. older).
- To assess relationships between the classic FADE score or the FADE-SAME score and other variables associated with age-related memory decline, we computed correlations with age, memory performance and hippocampal volume within age groups.
  - As an estimate of memory performance, we calculated the area under the ROC curve ( $A'$ ) from the performance in the memory task performed 70 min after the fMRI experiment (see Appendix B for details).
  - For estimation of hippocampal volumes ( $V_{HC}$ ), individuals' hippocampal volumes (in  $\text{mm}^3$ ) were obtained via automatic segmentation with FreeSurfer (Fischl, 2012) and the module for the segmentation of hippocampal subfields and amygdala nuclei (Iglesias et al., 2015; Saygin et al., 2017), which is robust across age groups and MRI scanners (Quattrini et al., 2020)(see Appendix C for details).
- We additionally performed two-sample t-tests between our cohort of young subjects and an independent replication cohort of young subjects (see Section 2.10) in order to assess stability of the scores for young subjects across studies.

- Finally, we calculated correlation coefficients for the scores of older subjects, computed using the young subjects of the main experiment versus the replication subjects as reference, in order to assess stability of the scores for older subjects.

### **2.10. Replication with an independent baseline cohort**

The paradigm employed in the present study had previously been used in a cohort of young adults (Assmann et al., 2020) (hence termed *yFADE*) consisting of 117 young subjects (60 male, 57 female, age range 19-33, mean age  $24.37 \pm 2.60$  years). In the present study, we used those separate young subjects for stability analyses, i.e. (i) to assess whether FADE-classic and FADE-SAME scores are comparable when calculated for young subjects from different cohorts and (ii) to assess whether the two FADE scores are comparable when calculated for older subjects using reference maps from different sets of young subjects.

### 3. Results

#### 3.1. Age-related differences in the human memory network could be replicated

Using two-sample t-tests, we compared the age-related activation differences during novelty processing (novel vs. master images) and successful encoding (parametric modulator of the novelty regressor with encoding success). Replicating previous studies (Maillet & Rajah, 2014), we found older participants to exhibit lower activation of inferior and medial temporal structures, particularly of the PHC, but relatively reduced deactivations in midline structures of the DMN during both novelty processing and successful encoding (see Figure 2).

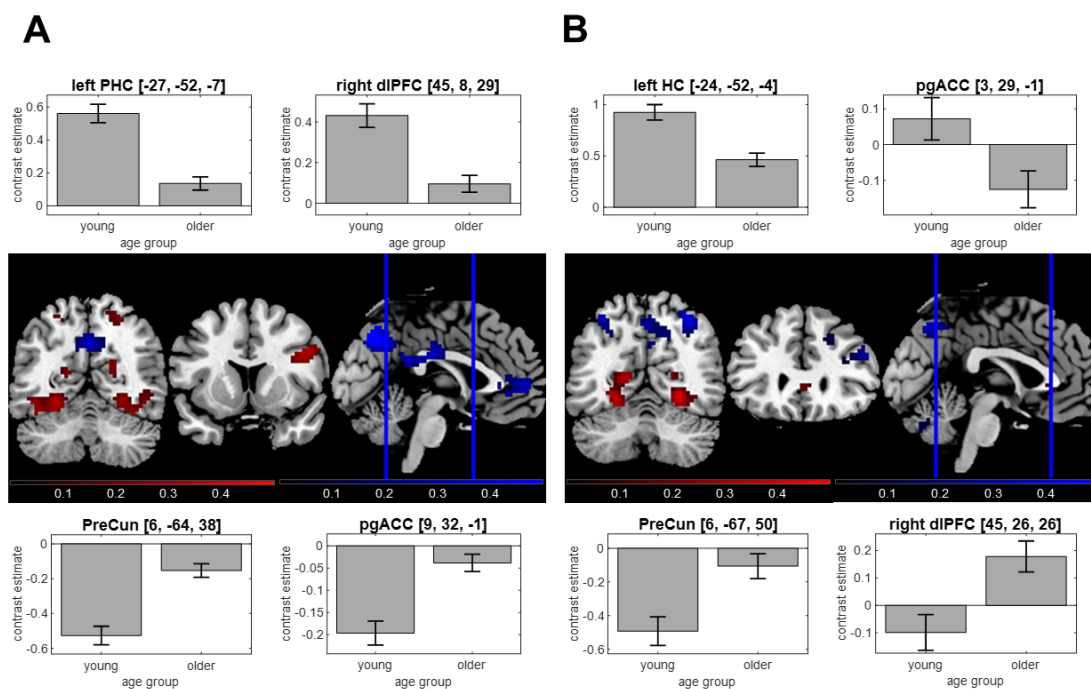


**Figure 2.** Age-related differences in the human memory network. Using our fMRI memory paradigm, we assessed novelty contrast and memory contrast and compared them between young and older adults. Brain sections show significant differences for activations (red) and deactivations (blue) in young subjects. Bar plots show group-level contrast estimates (gray) and 90% confidence intervals. (A) Significant effects of age on the novelty contrast, with reduced activations in PHC and dlPFC and reduced deactivations in PreCun and pgACC. (B) Significant effects of age on the memory contrast, with reduced activations in PHC and pgACC and reduced deactivations in PreCun and dlPFC.

#### 3.2. FADE scores are modulated by age, but neither gender nor MRI scanner

We first computed 2x2x2 ANOVAs to assess how the different FADE scores of the 217 subjects in our sample were influenced by (i) the two different age groups (young or older),

(ii) gender (male or female) and (iii) the MRI scanners in which they were investigated (Siemens Verio or Skyra; see Section 3.3).

There was a significant main effect of age group for all scores, except for the classic FADE score computed from the novelty contrast, which did not significantly differ between age groups (see Table 1). There were no main effects of scanner, gender, or interactions with them on any of the scores (see Table 1).

	novelty contrast		memory contrast	
	FADE score	SAME score	FADE score	SAME score
main effect of scanner	F = 0.11, p = 0.742	F = 0.14, p = 0.707	F = 0.13, p = 0.723	F = 1.65, p = 0.201
main effect of gender	F = 0.22, p = 0.636	F = 1.41, p = 0.236	F = 0.36, p = 0.550	F = 2.67, p = 0.104
main effect of age group	F = 0.16, p = 0.686	F = 16.56, p < 0.001	F = 81.76, p < 0.001	F = 135.04, p < 0.001
interaction of scanner and gender	F = 0.05, p = 0.815	F = 0.00, p = 0.999	F = 0.06, p = 0.810	F = 0.20, p = 0.653
interaction of scanner and age group	F = 1.84, p = 0.177	F = 0.02, p = 0.900	F = 0.97, p = 0.325	F = 0.71, p = 0.399
interaction of gender and age group	F = 2.10, p = 0.149	F = 0.01, p = 0.908	F = 0.44, p = 0.507	F = 0.84, p = 0.360
interaction of age group, scanner, and gender	F = 0.40, p = 0.528	F = 0.05, p = 0.826	F = 0.00, p = 0.995	F = 0.03, p = 0.853

**Table 1.** *Between-subject ANOVAs for FADE-classic and FADE-SAME scores.* Results from three-way ANOVAs with scanner, gender and age group as factors for both scores computed from both, novelty and memory contrast. All F-values have one numerator degree of freedom and 209 denominator degrees of freedom.

### 3.3. FADE scores differ in their ability to capture age-related differences

In order to directly compare the modulation of the two scores by age, we additionally computed 2x2 mixed ANOVAs with score (FADE-classic, FADE-SAME) as within-subject factor and age group (young, older) as between-subject factor, separately for the novelty and memory contrasts. There was a significant interaction between score and age for the novelty and memory contrast (see Table 2), supported by larger differences between age groups for the FADE-SAME score. Both scores showed robust age-group-related differences for the memory contrast, and the FADE-SAME score additionally exhibited age-group-related differences for the novelty contrast (see Figure 3).

Due to its construction (see Figure 1), the FADE-SAME score was zero on average for young subjects – because their activation patterns were by definition distributed around the reference

activities – and negative on average for older subjects – from summing up activation losses and reduced deactivations. Consequently, the FADE-SAME score was not significantly different from zero across the cohort of young subjects, whereas the negative values in the cohort of older subjects indicates a larger deviation of those individuals’ brain responses from the activation pattern in young subjects (see Figure 3).

When performing the same mixed ANOVAs, but this time comparing older subjects with middle-aged subjects (age range: 51-59 years) instead of young subjects, we found no significant differences between older and middle-aged subjects for any of the scores (see Supplementary Table S2 and Supplementary Figure S1).

	novelty contrast	memory contrast
main effect of age	F = 21.66, p < 0.001	F = 62.85, p < 0.001
main effect of score	F = 44.00, p < 0.001	F = 0.08, p = 0.783
interaction of age and score	F = 26.88, p < 0.001	F = 124.95, p < 0.001

**Table 2.** Within-subject ANOVAs for FADE-classic and FADE-SAME scores. Results from two-way ANOVAs with age group and fMRI score for both, novelty and memory contrast. All F-values have one numerator degree of freedom and 215 denominator degrees of freedom.

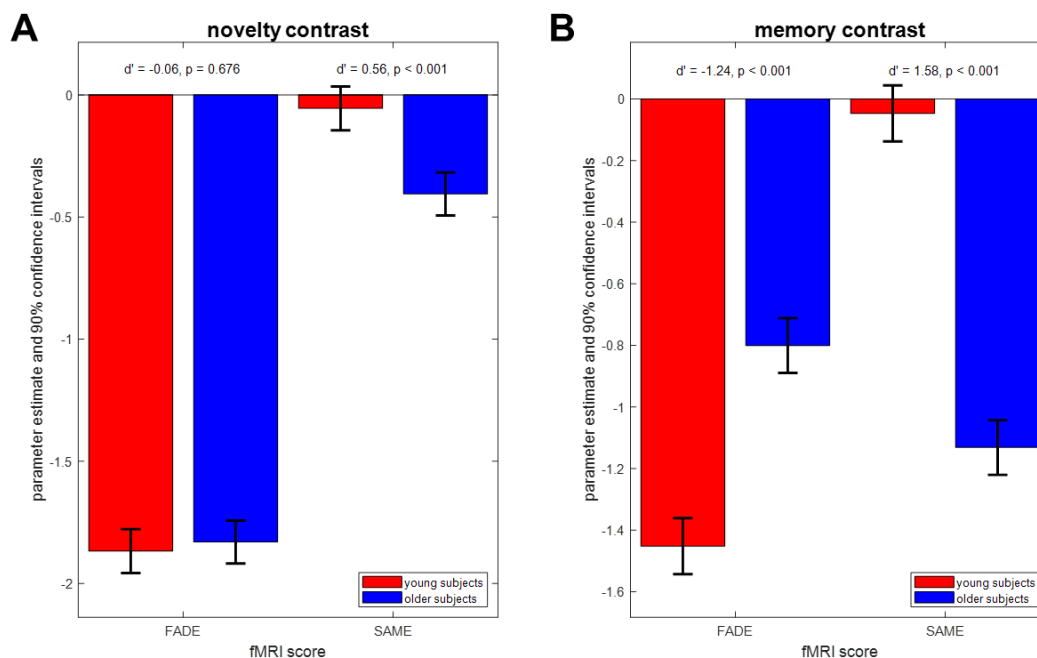


**Figure 3.** Differences of FADE-classic and FADE-SAME score between age groups. Results from mixed ANOVAs with fMRI score and age group as factors. (A) Parameter estimates and 90% confidence intervals for the novelty contrast. The FADE-SAME score shows an age group difference not found for the classic FADE score. (B) Parameter estimates and 90% confidence intervals for the memory contrast. Both the classic FADE score and the FADE-SAME score showed pronounced age-related differences.



### **3.4. FADE scores correlate with other indices of cognitive aging**

As described above, the classic FADE score for the memory contrast as well as both FADE-SAME scores differed significantly between age groups. Consequently, these scores were also correlated with age as a continuous variable (FADE-SAME based on memory contrast:  $r = -0.63$ ,  $p < 0.001$ ). However, when controlling for age group, namely calculating separate correlation coefficients for young and older subjects, those correlations were either very low (FADE scores based on memory contrast within older subjects) or not significant (all other scores; see Figure 4, 1<sup>st</sup> row). Moreover, there were significant correlations with memory performance, as measured by area under the curve (AUC), for the FADE-SAME score and for the classic FADE score computed from the memory contrast (see Figure 4C, D, 2<sup>nd</sup> row). For the novelty contrast, we observed a significant correlation of the FADE-SAME score, but not of the classic FADE score, with memory performance in older subjects (Figure 4B, 2<sup>nd</sup> row). No significant correlations with hippocampal volume could be observed for any of the scores (all  $p > 0.05$ ; see Figure 4, 3<sup>rd</sup> and 4<sup>th</sup> row).

To further explore the relationship between FADE scores and chronological age, we plotted the scores as a continuous function of age in years, highlighting that the age dependence of the scores reflects a group effect rather than a continuous relationship with age (see Supplementary Figure S2). In analogy to the correlational analyses depicted in Figure 4, we also report correlations between FADE scores and indices of cognitive aging in the middle-aged subjects ( $N = 42$ ) and in the young subjects ( $N = 117$ ) from our replication cohort (see Supplementary Figure S3).

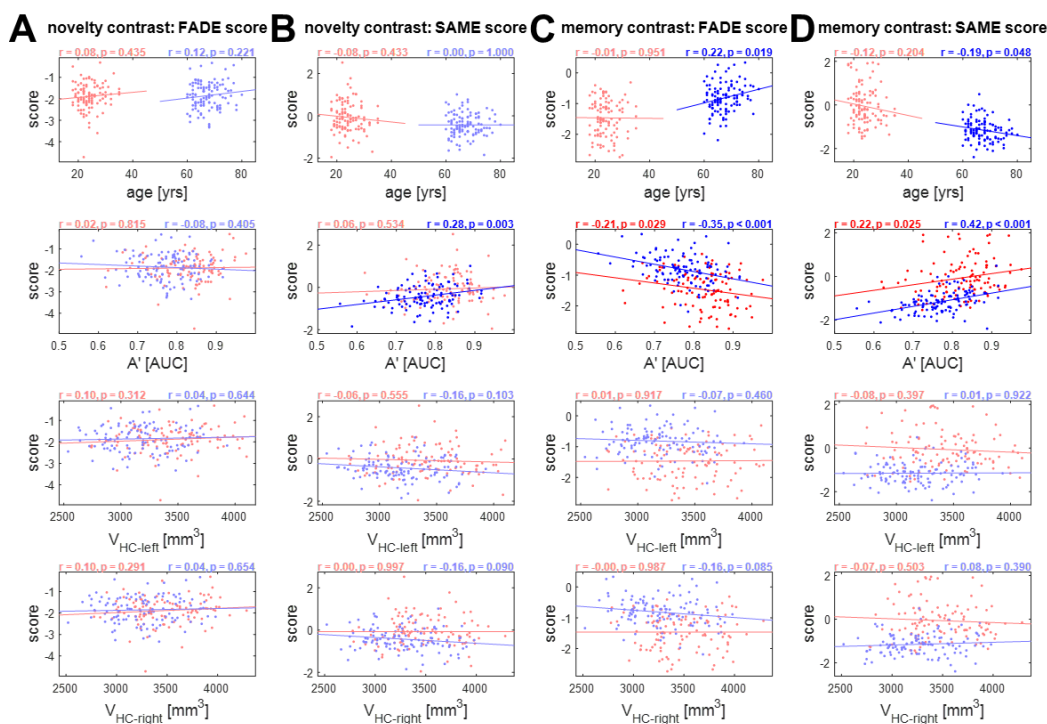


**Figure 4.** Correlations with independent variables, separated by age group. Results from correlation analyses of FADE-classic and FADE-SAME scores with age, memory performance ( $A'$ ) and hippocampal volumes ( $V_{HC}$ ). Correlations are reported separately for (A) the classic FADE score computed from the novelty contrast, (B) the FADE-SAME score computed from the novelty contrast, (C) the classic FADE score computed from the memory contrast and (D) the FADE-SAME score computed from the memory contrast. Young subjects are depicted in red, and older subjects are depicted in blue. Significant correlation coefficients are highlighted.

### 3.5. The FADE-SAME score is stable across different cohorts of young subjects

In order to test stability of FADE-classic and FADE-SAME score for young adults, we compared scores obtained from the 106 young subjects in our study sample (see Section 2.1) with scores obtained from the 117 young subjects in the replication cohort (see Section 2.10). Both sets of scores were obtained in a cross-validated fashion, such that all scores were computed using reference maps obtained from independent subjects, but from the same cohort (see Section 2.8).

FADE-SAME scores were close to zero on average by definition (as explained in Section 3.3) and did not differ significantly between original and replication subjects (see Figure 5B/D), whereas classic FADE scores showed significant group differences with small to medium effect sizes for novelty and memory contrast (see Figure 5A/C). Note that both cohorts were comparable regarding age range, mean age, and ratio of male to female participants (see Supplementary Table S1 and Section 2.10).

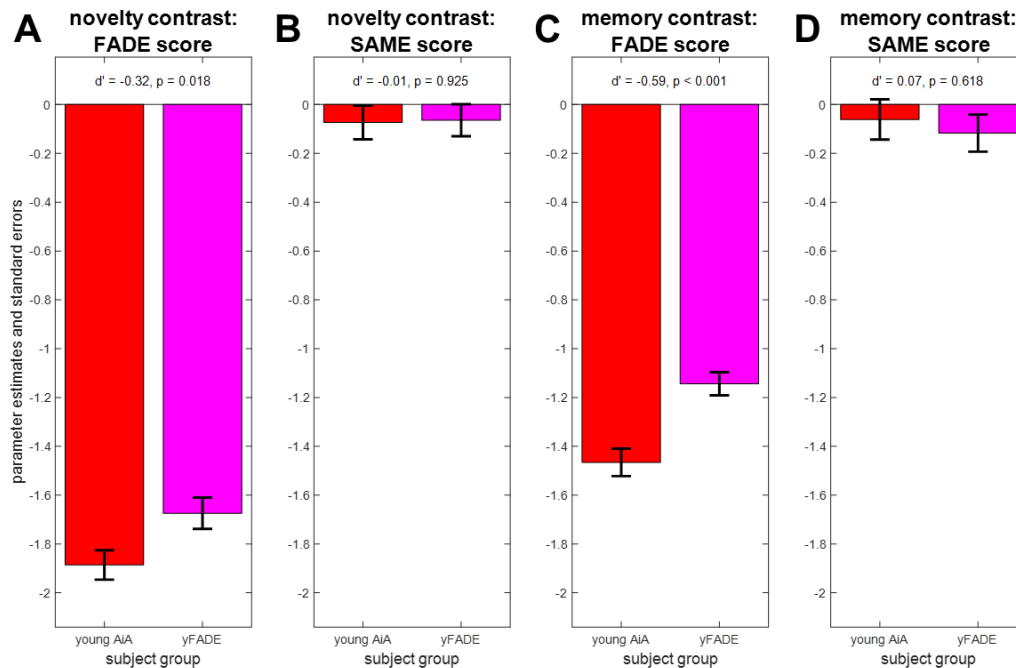


**Figure 5.** *Stability of the FADE scores for young subjects from different studies.* Comparison of original young subjects (young AiA, red) and replication young subjects (yFADE, magenta). **(A)** Classic FADE score computed from the novelty contrast. **(B)** FADE-SAME score computed from the novelty contrast. **(C)** Classic FADE score computed from the memory contrast. **(D)** FADE-SAME score computed from the memory contrast. There are no group differences for the FADE-SAME score (B, D), but significant differences between original and replication subjects for the classic FADE score (A, C).

### 3.6. FADE scores are stable for older subjects when using different reference samples

For future use of the classic FADE or FADE-SAME scores in the investigation of older adults and clinical populations, it is important to assess their generalizability, which is, among other factors, determined by their independence from the underlying reference sample. Therefore, we computed both scores for the 111 older subjects in our sample using reference maps (Figure 1A) obtained either from the young subjects of the main study sample or obtained from the young subjects of the replication cohort. We then calculated Pearson's correlation coefficients between the scores calculated with the two different baseline samples.

We found all scores (FADE-classic vs. FADE-SAME x novelty vs. memory contrast) to be highly correlated with the respective scores calculated based on the yFADE sample as reference (all  $r > 0.96$ , all  $p < 0.001$ ; see Figure 6), indicating their robustness with respect to different reference samples.

In additional analyses, we investigated the correlation between scores computed using reference maps obtained from either all young subjects of one cohort (contrary to the cross-validation scheme used here) or just half of those subjects (roughly equivalent to the cross-

validation scheme used here), finding similarly high correlations (see Supplementary Figure S4).

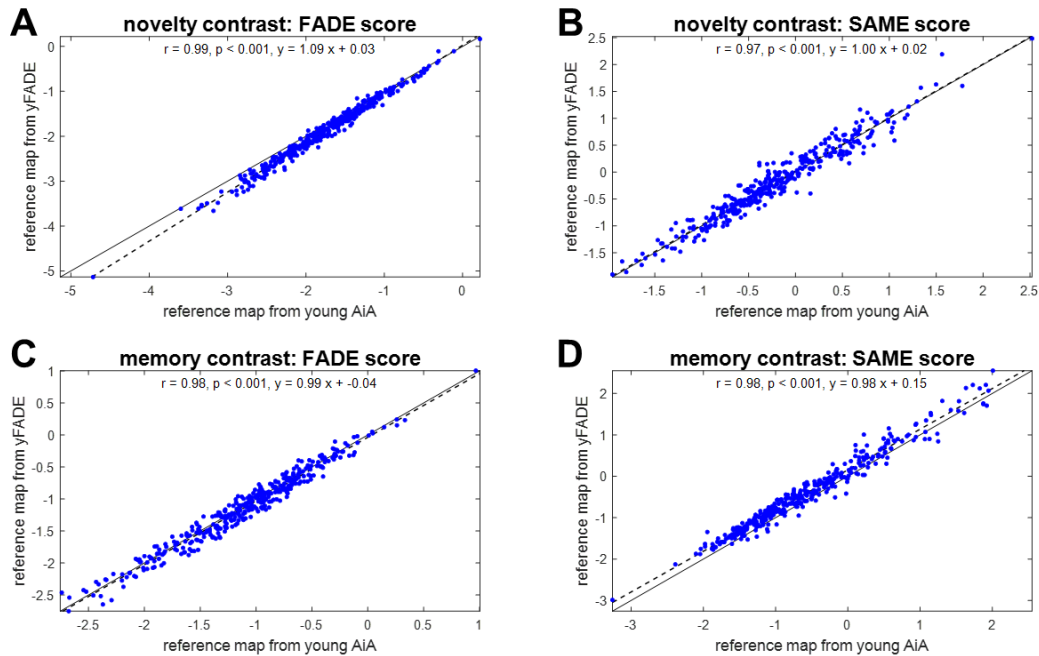


**Figure 6.** Stability of the FADE scores for older subjects as a function of reference sample. Comparison of scores computed for older subjects (older AiA), using reference maps obtained from either original young subjects (young AiA) or replication young subjects (yFADE). In all panels, the solid black line is the identity function, and the dashed black line represents the regression line. **(A)** Classic FADE score computed based on the novelty contrast. **(B)** FADE-SAME score computed based on the novelty contrast. **(C)** Classic FADE score computed based on the memory contrast. **(D)** FADE-SAME score computed based on the (parametric) memory contrast. There are highly significant correlations for both scores and both contrasts.

## 4. Discussion

In the study reported here, we have tested the utility of single-value scores of memory-related fMRI activation patterns as potential biomarkers for neurocognitive aging. To this end, we have developed the FADE-SAME score as an enhanced version of the classic FADE score (Düzel et al., 2011), thereby accounting for both individual differences in the baseline sample and the simultaneous presence of activations and deactivations. We then evaluated the two scores (FADE-classic, FADE-SAME), calculated from two different contrasts (novelty processing, subsequent memory) with respect to interpretability, correlation with age and other proxies of age-related memory decline (memory performance, hippocampal volumes) as well as their stability as a function of different reference samples.

### 4.1. Different FADE scores as biomarkers of the aging memory system

Based on the initial work introducing the FADE score as an efficient, reductionist measure of age-related alterations of the human MTL memory system (Düzel et al., 2011), we aimed to develop the FADE-SAME score as a more comprehensive measure of age-related changes. To this end, the FADE-SAME score takes into account variability of fMRI activity patterns across the cohort of young subjects used as a reference, and it incorporates differences in brain encoding-related brain responses in a more holistic way by considering differences in both activations and deactivations (Maillet & Rajah, 2014). Furthermore, we aimed to make the FADE-SAME score more interpretable by defining zero as a fixed value for normalcy, signifying the mean activation pattern of the baseline cohort of young adults.

These theoretical advantages come at the cost of being potentially more dependent on the baseline dataset. Specifically, computing a classic FADE score only requires a set of voxels showing a positive effect in a reference sample of young, healthy subjects. In contrast, computing a FADE-SAME score additionally requires average parameter estimates (i.e., beta values) from the reference set and their standard deviations. This could be a disadvantage of the FADE-SAME relative to the classic FADE score, as, compared to sets of significant voxels, estimated beta values may be more strongly dependent on nuisance variables like different MRI scanners, scanning and preprocessing parameters, or population effects of the chosen baseline sample. All of these factors could, in theory, limit the applicability of FADE-SAME scores for older adults based on activation templates obtained from another study.

Therefore, we aimed to assess the robustness of the different FADE scores with respect to different baseline samples. We calculated scores based on our current study sample and a

previously described sample (Assmann et al., 2020) that was demographically comparable, but investigated with slightly shorter trial timings as well as different scanning and preprocessing parameters (Soch et al., 2020). Notably, we observed uniformly strong correlations across the FADE scores based on the two different baseline samples, suggesting that, at least in the case of the present datasets, the aforementioned dependency of the FADE-SAME score on the baseline sample may be negligible in practice (see Figure 6).

For the FADE-SAME score to be employed as a potential biomarker, it is important that it does not merely bear advantages at the theoretical level, but works robustly in empirical investigations. Our validation analyses have indeed revealed highly encouraging empirical evidence regarding the practical utility of the FADE-SAME score. Firstly, the FADE-SAME score yielded a highly robust differentiation between the age groups of young and older subjects, particularly for the memory contrast, but also for the novelty contrast (see Figure 3 and discussion below). Similarly, when controlling for age group, the FADE-SAME score showed significant correlations with memory performance, not only when computed from the subsequent memory contrast, but also when computed from the novelty contrast (see Figure 4). The latter was not the case for the classic FADE score. Last, but not least, when computing FADE scores for the young subjects of our original cohort and the replication cohort, the FADE-SAME scores were associated high stability across subjects, yielding comparable values across the two samples (see Figure 5). This is particularly noteworthy when considering its computationally higher dependence on the reference sample. We suggest that this robustness with respect to the reference sample may be most readily explained by the fact that spurious activations at group level attributable to atypical individual activation patterns (M. B. Miller et al., 2002) are weighted less strongly when accounting for the standard deviation at each voxel.

#### **4.2. Novelty and subsequent memory contrasts as basis for the FADE scores**

While in the original study by Düzel and colleagues (Düzel et al., 2011), the FADE score was based on neural correlates of successful memory encoding, namely, the DM effect, there is considerable neuroanatomical overlap between the DM effect and the *novelty effect*, which is obtained by comparing novel items to previously familiarized items (Soch et al., 2020). In a previous analysis of memory-related brain activity patterns in young and older adults, we have shown that the novelty processing and successful memory encoding engaged largely overlapping networks in the human brain (Soch et al., 2020, Fig. 6A). The analyses reported

here have revealed that the same holds true for the age-related activation differences with respect to these contrasts (see Figure 2).

The novelty effect can be computed independently of successful encoding, which may be advantageous in memory-impaired individuals, who have an insufficiently low number of later remembered items for the calculation of a DM effect. However, when computing the FADE-classic and FADE-SAME scores, we found that the FADE scores computed from the subsequent memory contrast showed substantially more robust age differences than those obtained from the novelty contrast. In fact, the classic FADE score computed from the novelty contrast did not discriminate significantly between young and older participants (see Table 2 and Figure 3). This observation was somewhat unexpected, as novelty-related hippocampal activation has already been negatively associated with Tau protein concentrations in the CSF of older adults (Düzel et al., 2018). On the other hand, the FADE scores likely constitute more comprehensive indices of neurocognitive aging than isolated hippocampal activation differences (see Section 3.3).

Two notable exceptions to the overall strong overlap of the age-related activation differences of novelty and subsequent memory contrasts are the right dlPFC and the anterior cingulate cortex (pgACC). The right dlPFC shows a negative effect of age on novelty (i.e. higher activations for young subjects), but a positive effect of age on memory (i.e. higher activations for older subjects), while the pgACC shows a positive effect of age on novelty, but a negative effect of age on memory (see Figure 2). However, these findings do not seem to contradict the general rule that a region characterized by activations in young subjects shows lower activity in older subjects and that a region characterized by deactivations in young subjects shows reduced deactivations or even absolute activations (relative to baseline) in older subjects (see Figure 2).

#### **4.3.Reductionist versus multi-voxel fMRI activation scores as potential biomarkers**

Since the first description of the FADE score (Düzel et al., 2011), relatively few studies have used fMRI correlates of memory processes as indices of cognitive aging at the individual level. One study revealed a relationship of dedifferentiation of stimulus-specific processing in the lateral occipital cortex and parahippocampal place area and memory performance (Koen et al., 2019), but in that study, age and memory performance were independently associated with dedifferentiation (for a further discussion, see Koen and Rugg, 2019). Recently, recollection-related fMRI activation of the hippocampus during retrieval has been associated with both memory performance and longitudinal preservation of memory performance in

older adults (Hou et al., 2020). While this approach will likely yield similar results to our whole-brain approach with encoding-related activation patterns, it may be limited in subjects with very poor memory performance, like individuals with subjective cognitive decline or mild cognitive impairment, especially considering that an associative word-pair learning task was used. Furthermore, the utility of focusing on the hippocampus may be limited by the strong task-dependency of hippocampal activation. Prior research has shown a positive relationship between higher hippocampal integrity and increased activation signaling during novelty processing (Düzel et al., 2018), but – potentially compensatory – over-recruitment and thus more pronounced deviation from the prototypical activation patterns during encoding compared to a low-level baseline (Bookheimer et al., 2000), or during pattern separation (Bakker et al., 2012; Berron et al., 2019).

Irrespective of the specific statistic employed, the current practice for establishing memory-related fMRI activations as a potential biomarker is still to compute a summary statistic from an fMRI contrast (e.g., hippocampal activation or a FADE-score-type statistic). The usual aim is that this statistic is linearly related to some clinically relevant variable such as age, memory performance, or grey matter density (see Figure 7A). More recently, partial least squares (PLS)-based decomposition of memory-related fMRI activations has been employed as a whole-brain multivariate approach to identify indices of pathological aging and dementia risk (Rabipour et al., 2020). In the ongoing search for a memory-related fMRI biomarker with the potential to make predictions at the single-subject level, future studies will be needed to directly compare multivariate and reductionist approaches.

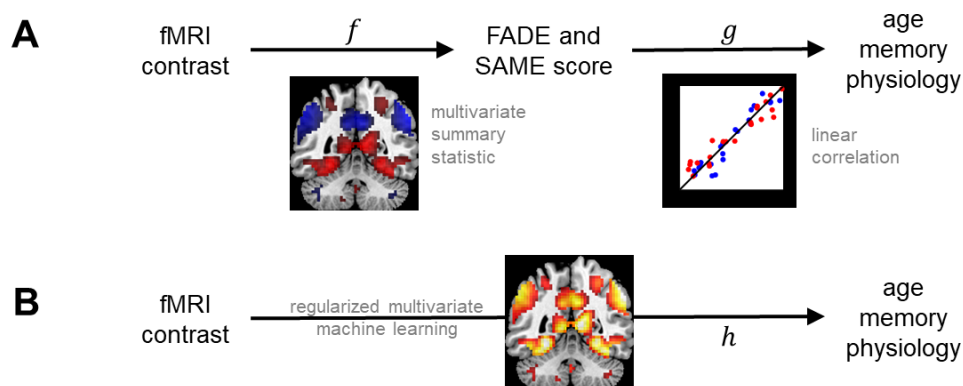


**Figure 7.** Employing fMRI contrasts to predict human phenotypes. (A) Current approach to predicting phenotype from fMRI. A function  $f$  is calculated from a voxel-wise fMRI contrast map and it is tested whether there is a linear mapping  $g$  from the outcome of this function to variables of interest. (B) Envisaged approach to predicting phenotype from fMRI. The non-linear mapping  $h$  from voxel-wise fMRI contrast to human phenotype is directly estimated using an advanced machine learning technique.



In this context, a potentially more sensitive approach might be to directly predict the variable of interest from the voxel-wise fMRI contrast using some regularized multivariate machine learning method (see Figure 7B). Such a method (i) will be based on machine learning, because the precise mapping function is not known *a priori* and (ii) will use regularization, because the number of features (i.e., voxels) is much larger than the number of observations (i.e., patients or healthy older adults) used to train the mapping. For example, one could apply support vector classification (SVC) to decode age group or disease state from estimated fMRI activity; or support vector regression (SVR) to find a non-linear mapping between estimated fMRI activity and observed memory performance, conditional on age.

#### **4.4. Clinical implications and directions for future research**

In the present study, we restricted our analyses to a neurologically healthy population, and the observed individual differences in the FADE scores therefore most likely reflect physiological interindividual variability in age-related alterations of the MTL memory system and associated brain networks. In clinical research, the utility of a biomarker depends on its ability to discriminate (i) between healthy controls and affected individuals, or (ii) between different pathophysiological underpinnings of an observed clinical entity. While we were able to show that the evaluated highly reductionist and easy-to-use scores reliably detect correlates of age-related alterations in human explicit memory networks, they will yet need to prove their suitability to discriminate, for example, between cognitively impaired individuals with and without underlying Alzheimer's disease pathology (Jessen et al., 2018).

In this context, one question of potentially high clinical relevance will be to what extent the two scores investigated in the present study may correlate with different stages of Alzheimer's pathology. The classic FADE score constitutes a sum score reflecting reduced activations of the MTL memory system, whereas the FADE-SAME score additionally accounts for age-related hyperactivation (or reduced deactivation) of the brain's midline structures that constitute the Default Mode Network (Maillet & Rajah, 2014). In AD, deposition of Tau protein aggregates typically starts in the MTL and subsequently spreads to the brain's midline. Recently, patterns of Tau deposition could be linked to distinct impairment of item memory versus scene memory (Maass et al., 2019). Future research should thus assess to what extent the scores might differentially reflect MTL versus midline pathology in individuals with AD.

#### **4.5. Conclusion**

We could demonstrate that single-value scores reflecting age-related deviations from prototypical fMRI activations during memory encoding bear the potential to be used as biomarkers of cognitive aging. Moreover, the FADE-SAME score could also differentiate between age groups when computed from the novelty contrast, suggesting its suitability in memory-impaired clinical populations. In the future, single-value scores reflecting fMRI responses may help to identify distinct subtypes of age-related memory decline and pathological alterations of human memory systems.

## 5. References

- Ackenheil, M., Stotz, G., Dietz-Bauer, R., & Vossen, A. (1999). *Mini International Neuropsychiatric Interview - German version 5.0.0*. Psychiatrische Universitätsklinik.
- Assmann, A., Richter, A., Schütze, H., Soch, J., Barman, A., Behnisch, G., Knopf, L., Raschick, M., Schult, A., Wüstenberg, T., Behr, J., Düzel, E., Seidenbecher, C. I., & Schott, B. H. (2020). Neurocan genome-wide psychiatric risk variant affects explicit memory performance and hippocampal function in healthy humans. *European Journal of Neuroscience*, February, ejn.14872. <https://doi.org/10.1111/ejn.14872>
- Bainbridge, W. A., Berron, D., Schütze, H., Cardenas-Blanco, A., Metzger, C., Dobisch, L., Bittner, D., Glanz, W., Spottke, A., Rudolph, J., Brosseron, F., Buerger, K., Janowitz, D., Fliessbach, K., Heneka, M., Laske, C., Buchmann, M., Peters, O., Diesing, D., ... Düzel, E. (2019). Memorability of photographs in subjective cognitive decline and mild cognitive impairment: Implications for cognitive assessment. *Alzheimer's and Dementia: Diagnosis, Assessment and Disease Monitoring*, 11, 610–618. <https://doi.org/10.1016/j.dadm.2019.07.005>
- Bakker, A., Krauss, G. L., Albert, M. S., Speck, C. L., Jones, L. R., Stark, C. E., Yassa, M. A., Bassett, S. S., Shelton, A. L., & Gallagher, M. (2012). Reduction of hippocampal hyperactivity improves cognition in amnesic Mild Cognitive Impairment. *Neuron*, 74(3), 467–474. <https://doi.org/10.1016/j.neuron.2012.03.023>
- Barman, A., Assmann, A., Richter, S., Soch, J., Schäfer, H., Wüstenberg, T., Deibele, A., Klein, M., Richter, A., Behnisch, G., Düzel, E., Zenker, M., Seidenbecher, C. I., & Schott, B. H. (2014). Genetic variation of the RASGRF1 regulatory region affects human hippocampus-dependent memory. *Frontiers in Human Neuroscience*, 8(1 APR), 1–12. <https://doi.org/10.3389/fnhum.2014.00260>
- Berron, D., Cardenas-Blanco, A., Bittner, D., Metzger, C. D., Spottke, A., Heneka, M. T., Fliessbach, K., Schneider, A., Teipel, S. J., Wagner, M., Speck, O., Jessen, F., & Düzel, E. (2019). Higher CSF Tau Levels Are Related to Hippocampal Hyperactivity and Object Mnemonic Discrimination in Older Adults. *The Journal of Neuroscience*, 39(44), 8788–8797. <https://doi.org/10.1523/JNEUROSCI.1279-19.2019>
- Bookheimer, S. Y., Strojwas, M. H., Cohen, M. S., Saunders, A. M., Pericak-Vance, M. A., Mazziotta, J. C., & Small, G. W. (2000). Patterns of Brain Activation in People at Risk for Alzheimer's Disease. *New England Journal of Medicine*, 343(7), 450–456. <https://doi.org/10.1056/NEJM200008173430701>
- Brewer, J. B. (1998). Making Memories: Brain Activity that Predicts How Well Visual Experience Will Be Remembered. *Science*, 281(5380), 1185–1187. <https://doi.org/10.1126/science.281.5380.1185>
- Dounavi, M.-E., Mak, E., Wells, K., Ritchie, K., Ritchie, C. W., Su, L., & O' Brien, J. T. (2020). Volumetric alterations in the hippocampal subfields of subjects at increased risk of dementia. *Neurobiology of Aging*, 91, 36–44. <https://doi.org/10.1016/j.neurobiolaging.2020.03.006>
- Düzel, E., Acosta-Cabronero, J., Berron, D., Biessels, G. J., Björkman-Burtscher, I., Bottlaender, M., Bowtell, R., Buchem, M. v., Cardenas-Blanco, A., Boumezbuer, F., Chan, D., Clare, S., Costagli, M., Rochefort, L., Fillmer, A., Gowland, P., Hansson, O., Hendrikse, J., Kraff, O., ... Speck, O. (2019). European Ultrahigh-Field Imaging Network for Neurodegenerative Diseases (EUFIND). *Alzheimer's & Dementia: Diagnosis, Assessment & Disease Monitoring*, 11(1), 538–549.

<https://doi.org/10.1016/j.dadm.2019.04.010>

- Düzel, E., Berron, D., Schütze, H., Cardenas-Blanco, A., Metzger, C., Betts, M., Ziegler, G., Chen, Y., Dobisch, L., Bittner, D., Glanz, W., Reuter, M., Spottke, A., Rudolph, J., Brosseron, F., Buerger, K., Janowitz, D., Fliessbach, K., Heneka, M., ... Jessen, F. (2018). CSF total tau levels are associated with hippocampal novelty irrespective of hippocampal volume. *Alzheimer's & Dementia: Diagnosis, Assessment & Disease Monitoring*, *10*(1), 782–790. <https://doi.org/10.1016/j.dadm.2018.10.003>
- Düzel, E., Schütze, H., Yonelinas, A. P., & Heinze, H.-J. (2011). Functional phenotyping of successful aging in long-term memory: Preserved performance in the absence of neural compensation. *Hippocampus*, *21*, 803–814. <https://doi.org/10.1002/hipo.20834>
- Fischl, B. (2012). FreeSurfer. *NeuroImage*, *62*(2), 774–781. <https://doi.org/10.1016/j.neuroimage.2012.01.021>
- Hou, M., de Chastelaine, M., Jayakumar, M., Donley, B. E., & Rugg, M. D. (2020). Recollection-related hippocampal fMRI effects predict longitudinal memory change in healthy older adults. *Neuropsychologia*, *146*, 107537. <https://doi.org/10.1016/j.neuropsychologia.2020.107537>
- Iglesias, J. E., Augustinack, J. C., Nguyen, K., Player, C. M., Player, A., Wright, M., Roy, N., Frosch, M. P., McKee, A. C., Wald, L. L., Fischl, B., & Van Leemput, K. (2015). A computational atlas of the hippocampal formation using ex vivo, ultra-high resolution MRI: Application to adaptive segmentation of in vivo MRI. *NeuroImage*, *115*, 117–137. <https://doi.org/10.1016/j.neuroimage.2015.04.042>
- Jessen, F., Spottke, A., Boecker, H., Brosseron, F., Buerger, K., Catak, C., Fliessbach, K., Franke, C., Fuentes, M., Heneka, M. T., Janowitz, D., Kilimann, I., Laske, C., Menne, F., Nestor, P., Peters, O., Priller, J., Pross, V., Ramirez, A., ... Düzel, E. (2018). Design and first baseline data of the DZNE multicenter observational study on pre-dementia Alzheimer's disease (DELCODE). *Alzheimer's Research and Therapy*, *10*(1), 1–10. <https://doi.org/10.1186/s13195-017-0314-2>
- Kim, H. (2011). Neural activity that predicts subsequent memory and forgetting: A meta-analysis of 74 fMRI studies. *NeuroImage*, *54*(3), 2446–2461. <https://doi.org/10.1016/j.neuroimage.2010.09.045>
- Koen, J. D., Hauck, N., & Rugg, M. D. (2019). The relationship between age, neural differentiation, and memory performance. *Journal of Neuroscience*, *39*(1), 149–162. <https://doi.org/10.1523/JNEUROSCI.1498-18.2018>
- Koen, J. D., & Rugg, M. D. (2019). Neural Dedifferentiation in the Aging Brain. *Trends in Cognitive Sciences*, *23*(7), 547–559. <https://doi.org/10.1016/j.tics.2019.04.012>
- Maass, A., Berron, D., Harrison, T. M., Adams, J. N., La Joie, R., Baker, S., Mellinger, T., Bell, R. K., Swinnerton, K., Inglis, B., Rabinovici, G. D., Düzel, E., & Jagust, W. J. (2019). Alzheimer's pathology targets distinct memory networks in the ageing brain. *Brain*, *142*(8), 2492–2509. <https://doi.org/10.1093/brain/awz154>
- Maillet, D., & Rajah, M. N. (2014). Age-related differences in brain activity in the subsequent memory paradigm: A meta-analysis. *Neuroscience and Biobehavioral Reviews*, *45*, 246–257. <https://doi.org/10.1016/j.neubiorev.2014.06.006>
- Miller, M. B., Van Horn, J. D., Wolford, G. L., Handy, T. C., Valsangkar-Smyth, M., Inati, S., Grafton, S., & Gazzaniga, M. S. (2002). Extensive Individual Differences in Brain Activations Associated with Episodic Retrieval are Reliable Over Time. *Journal of Cognitive Neuroscience*, *14*(8), 1200–1214.

<https://doi.org/10.1162/089892902760807203>

- Miller, S. L., Celone, K., DePeau, K., Diamond, E., Dickerson, B. C., Rentz, D., Pihlajamaki, M., & Sperling, R. A. (2008). Age-related memory impairment associated with loss of parietal deactivation but preserved hippocampal activation. *Proceedings of the National Academy of Sciences*, *105*(6), 2181–2186. <https://doi.org/10.1073/pnas.0706818105>
- Paller, K. A., Kutas, M., & Mayes, A. R. (1987). Neural correlates of encoding in an incidental learning paradigm. *Electroencephalography and Clinical Neurophysiology*, *67*(4), 360–371. [https://doi.org/10.1016/0013-4694\(87\)90124-6](https://doi.org/10.1016/0013-4694(87)90124-6)
- Quattrini, G., Pievani, M., Jovicich, J., Aiello, M., Bargalló, N., Barkhof, F., Bartres-Faz, D., Beltramello, A., Pizzini, F. B., Blin, O., Bordet, R., Caulo, M., Constantinides, M., Didic, M., Drevelegas, A., Ferretti, A., Fiedler, U., Floridi, P., Gros-Dagnac, H., ... Marizzoni, M. (2020). Amygdalar nuclei and hippocampal subfields on MRI: Test-retest reliability of automated volumetry across different MRI sites and vendors. *NeuroImage*, *218*(May). <https://doi.org/10.1016/j.neuroimage.2020.116932>
- Rabipour, S., Rajagopal, S., Pasvanis, S., Group, P.-A. R., & Rajah, M. N. (2020). Dedifferentiation of memory-related brain function as a potential early biomarker of Alzheimer's disease in asymptomatic older women: Results from the PREVENT-AD Cohort. *MedRxiv*. <https://doi.org/10.1101/2020.11.30.20241117>
- Saygin, Z. M., Kliemann, D., Iglesias, J. E., van der Kouwe, A. J. W., Boyd, E., Reuter, M., Stevens, A., Van Leemput, K., McKee, A., Frosch, M. P., Fischl, B., & Augustinack, J. C. (2017). High-resolution magnetic resonance imaging reveals nuclei of the human amygdala: manual segmentation to automatic atlas. *NeuroImage*, *155*, 370–382. <https://doi.org/10.1016/j.neuroimage.2017.04.046>
- Schott, B. H., Assmann, A., Schmierer, P., Soch, J., Erk, S., Garbusow, M., Mohnke, S., Pöhland, L., Romanczuk-Seiferth, N., Barman, A., Wüstenberg, T., Haddad, L., Grimm, O., Witt, S., Richter, S., Klein, M., Schütze, H., Mühleisen, T. W., Cichon, S., ... Walter, H. (2014). Epistatic interaction of genetic depression risk variants in the human subgenual cingulate cortex during memory encoding. *Translational Psychiatry*, *4*(3), e372–e372. <https://doi.org/10.1038/tp.2014.10>
- Sheehan, D. V., Lecrubier, Y., Sheehan, H., Amorim, P., Janavs, J., Weiller, E., Hergueta, T., Baker, R., & Dunbar, G. C. (1998). The Mini-International Neuropsychiatric Interview (M.I.N.I.): the development and validation of a structured diagnostic psychiatric interview for DSM-IV and ICD-10. *Journal of Clinical Psychiatry*, *59*(Suppl 20), 22–33.
- Soch, J., Richter, A., Schütze, H., Kizilirmak, J. M., Assmann, A., Knopf, L., Raschick, M., Schult, A., Maass, A., Ziegler, G., Richardson-Klavehn, A., Düzel, E., & Schott, B. H. (2020). Bayesian model selection favors parametric over categorical models of the fMRI subsequent memory effect in young and elderly adults. *BioRxiv*, 2020.07.27.220871.
- Wagner, A. D., Schacter, D. L., Rotte, M., Koutstaal, W., Maril, A., Dale, A. M., Rosen, B. R., & Buckner, R. L. (1998). Building memories: Remembering and forgetting of verbal experiences as predicted by brain activity. *Science*, *281*(5380), 1188–1191. <https://doi.org/10.1126/science.281.5380.1188>
- World Medical Association. (2013). World Medical Association Declaration of Helsinki: Ethical principles for medical research involving human subjects. *JAMA*, *310*(20), 2191–2194. <https://doi.org/10.1001/jama.2013.281053>

## 6. Appendix

### A. Interpretations of the FADE-SAME score

When simply spelling out the equation of the FADE-SAME score, it represents the sum of *average normalized activation loss* in voxels with positive effects and *average normalized deactivation loss* in voxels with negative effects (see Section 2.3):

$$\text{SAME}_i = \frac{1}{v_+} \sum_{j \in J_+} \frac{\hat{\gamma}_{ij} - \hat{\beta}_j}{\hat{\sigma}_j} + \frac{1}{v_-} \sum_{j \in J_-} \frac{\hat{\beta}_j - \hat{\gamma}_{ij}}{\hat{\sigma}_j}$$

If we focus on just one voxel  $j$ , then the variance-weighted Euclidean distance of an older adult's activation from the average young subject in this voxel is

$$\sqrt{\frac{(\hat{\gamma}_{ij} - \hat{\beta}_j)^2}{\hat{\sigma}_j^2}} = \frac{|\hat{\gamma}_{ij} - \hat{\beta}_j|}{\hat{\sigma}_j}$$

Since we want to obtain directional information (i.e., increased activation/deactivation should benefit while the same amount of decreased activation/deactivation should impair the FADE-SAME score), the activation difference is sign-adjusted for the reference effect

$$(\hat{\gamma}_{ij} - \hat{\beta}_j) \rightarrow \begin{cases} +(\hat{\gamma}_{ij} - \hat{\beta}_j) = \hat{\gamma}_{ij} - \hat{\beta}_j, & \text{if } \hat{\beta}_j > 0 \\ -(\hat{\gamma}_{ij} - \hat{\beta}_j) = \hat{\beta}_j - \hat{\gamma}_{ij}, & \text{if } \hat{\beta}_j < 0 \end{cases}$$

which renders the FADE-SAME score as the *voxel-averaged variance-adjusted directional Euclidean distance* of one subject's activations from the reference pattern.

Alternatively, one voxel's term from the sum over voxel sets

$$\frac{\hat{\gamma}_{ij} - \hat{\beta}_j}{\hat{\sigma}_j}$$

can be seen as an effect size estimate similar to Cohen's  $d$  (Cohen, 1988) where the difference of means (or estimated regression coefficients) is divided by the estimated standard deviation.

More precisely, the term is equivalent to Glass'  $\Delta$  (Glass, 1976)

$$\frac{\bar{x}_1 - \bar{x}_2}{s_2}$$

where  $\bar{x}_1$  is the estimate from the subject to be assessed (e.g., an older adult),  $\bar{x}_2$  is the average estimate from the control group (i.e., the young adults) and  $s_2$  is the standard deviation calculated from the control group. Taking this into account, the FADE-SAME score is equivalent to the *voxel-averaged directional effect size*.

## B. Computation of memory performance

Let  $o_1, \dots, o_5$  and  $n_1, \dots, n_5$  be the numbers of old stimuli and new stimuli, respectively, rated during retrieval as 1 (“definitely new”) to 5 (“definitely old”). Then, hit rates and false alarm (FA) rates as functions of a threshold  $t \in \{0, 1, \dots, 5\}$  are given as the proportions of old stimuli and new stimuli, respectively, rated higher than  $t$ :

$$H(t) = \frac{1}{O} \sum_{i=t+1}^5 o_i$$

$$FA(t) = \frac{1}{N} \sum_{i=t+1}^5 n_i$$

where  $O = o_1 + \dots + o_5$  and  $N = n_1 + \dots + n_5$ . Note that  $H(0) = FA(0) = 1$  and  $H(5) = FA(5) = 0$ . Consider the hit rate as a function of the FA rate:

$$y = f(x), \text{ such that } y = H(t) \text{ and } x = FA(t) \text{ for each } t = 0, 1, \dots, 5$$

Then, the area under the ROC curve is given as the integral of this function from 0 to 1:

$$A' = \int_0^1 f(x) dx = \int_0^1 H(FA) dFA$$

This quantity is referred to as “A-prime” and serves as a measure for memory performance: When the response to each item is random, such that  $o_1, \dots, o_5$  and  $n_1, \dots, n_5$  have a uniform distribution,  $A'$  is 0.5, corresponding to pure guessing. When all old items are recognized ( $o_5 = O$ ) and all new items are rejected ( $n_1 = N$ ),  $A'$  is 1, corresponding to perfect performance.

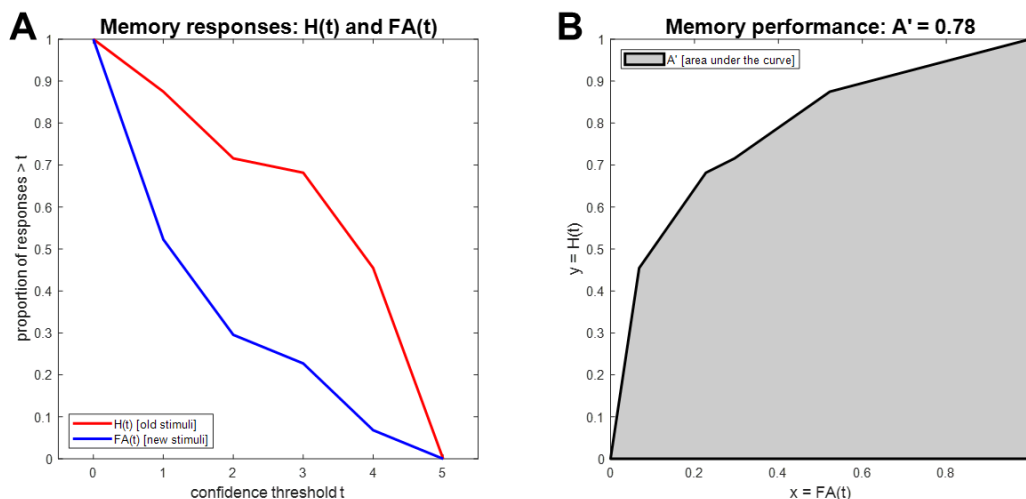


**Figure 8.** Calculation of  $A'$  as a measure of memory performance. **(A)** Hit rate (H) and false alarm (FA) rate are calculated from raw memory responses as a function of confidence threshold. **(B)** Memory performance is quantified as the area under the curve (AUC) when plotting hit rate against false alarm rate.

### **C. Computation of hippocampal volumes**

Hippocampi of individual participants were segmented using FreeSurfer 6.0 and the module for segmentation of hippocampal subfields and amygdalar nuclei<sup>3</sup>, following previous descriptions (Iglesias et al., 2015; Quattrini et al., 2020). In addition to the high-resolution T1-weighted images, high-resolution T2-weighted images acquired perpendicular to the hippocampal axis (see Section 2.3) were processed with the FreeSurfer pipeline, to improve segmentation accuracy (Dounavi et al., 2020). For the purpose of the present study, only the volume of the entire hippocampus, but no volumes of subfields were considered for analysis.

In the replication cohort (see Supplementary Figure S3), the segmentation with FreeSurfer 6.0 was performed based on T1-weighted MPRAGE images only, as no high-resolution T2-weighted MR images were available in that cohort.

---

<sup>3</sup> URL: <https://surfer.nmr.mgh.harvard.edu/fswiki/HippocampalSubfieldsAndNucleiOfAmygdala>.



## **7. Statements**

### **7.1. Acknowledgments**

The authors would like to thank Adriana Barman, Marieke Klein, Kerstin Möhring, Katja Neumann, Ilona Wiedenhöft, and Claus Tempelmann for assistance with MRI data acquisition. We further thank Constanze Seidenbecher and Gusalija Behnisch for support throughout the study.

### **7.2. Data Availability Statement**

Due to data protection regulations, sharing of the entire data set underlying this study in a public repository is not possible. We have previously provided GLM contrast images as a NeuroVault collection (<https://neurovault.org/collections/QBHNSRVW/>) with an earlier article using the same dataset (Soch et al., 2020), for a total of 217 (original cohort) + 42 (middle-aged subjects, see Supplementary Information) + 117 (replication cohort) subjects. Access to de-identified raw data will be provided by the authors upon reasonable request. MATLAB code and instructions to process the data can be found in an accompanying GitHub repository ([https://github.com/JoramSoch/FADE\\_SAME](https://github.com/JoramSoch/FADE_SAME)).

### **7.3. Funding and Conflict of Interest declaration**

This study was supported by the State of Saxony-Anhalt and the European Union (Research Alliance “Autonomy in Old Age”) and by the Deutsche Forschungsgemeinschaft (SFB 779, TP A08 and A10 to B.H.S.; DFG RI 2964-1 to A.R.). The funding agencies had no role in the design or analysis of the study. The authors have no conflict of interest, financial or otherwise, to declare.